Ceramics International 48 (2022) 22808–22819

Contents lists available at ScienceDirect

Ceramics International

journal homepage: www.elsevier.com/locate/ceramint

Characterization of titanium ceramic composite for bone implants applications

Lohashenpahan Shanmuganantha [a], Muhammad Umar Aslam Khan [b,c,d], Abu Bakar Sulong [e], Mohd Ikram Ramli [e], Azmi Baharudin [f], Hisam Muhamad Ariffin [f], Saiful Izwan Abd Razak [g], Min Hwei Ng [a,*]

[a] Department of Tissue Engineering, National University of Malaysia, Selangor Darul Ehsan, Malaysia
[b] BioInspired Device and Tissue Engineering Research Group, School of Biomedical Engineering and Health Sciences, Faculty of Engineering, Universiti Teknologi Malaysia, 81300, Skudai, Johor, Malaysia
[c] Institute for Personalized Medicine, School of Biomedical Engineering and Med-X Research Institute, Shanghai Jiao Tong University, 1954 Huashan Road, Shanghai, 200030, China
[d] Nanosciences and Technology Department (NS & TD), National Center for Physics, Quaid-i-Azam University Campus, Islamabad, 44000, Pakistan
[e] Department of Mechanical Engineering, National University of Malaysia, Selangor Darul, Ehsan, Malaysia
[f] Department of Orthopaedic and Traumatology, National University of Malaysia, Selangor Darul Ehsan, 56000, Malaysia
[g] Centre of Advanced Composite Materials, Faculty of Engineering, Universiti Teknologi Malaysia, 81300, Skudai, Johor, Malaysia

ARTICLE INFO

Keywords:
Titanium
Wollastonite
Bioceramic
Mesenchymal stem cells
Bone implants

ABSTRACT

Bone implants are widely used to restore bone loss due to several factors including but not limited to osteoporosis, osteoarthritis and road injuries. Current bone implant materials restore mechanical stability but suffer from a lack of osteointegration and will need to be replaced after long term use. To circumvent this, tissue engineering which capitalizes on the use of cells, biochemical factors and biodegradable materials aim to develop a biological substitute that restores, maintain or improve tissue functions. Central to the improvement of the tissue function and its stability through the implant relies on its interaction with the host tissue. Hence, a bioactive implant that promotes osteointegration is more desirable than an inert implant. In this study, metal-ceramic composites are explored for their suitability to be used as bone implants in the future. Fabrication of the composite was optimized using hot press compression and vacuum sintering method. Data presented include physicochemical characteristics of titanium-hydroxyapatite and titanium-wollastonite analyzed via SEM, FTIR, XRD, 3D laser microscopy and mechanical test. Evidence of material biocompatibility with primary human osteoprogenitor cells is also provided. Both titanium hydroxyapatite and titanium wollastonite possess the potential as the future of metal-ceramic composites as they possess the bioactivity of ceramic while still maintaining its core titanium body as a source of strength.

1. Introduction

Titanium has been widely used within the field of medicine as a metal for orthopaedic implants as it is mechanically stable and inert to any biological reactions. Many studies are still being carried out until this day to determine the effectiveness of titanium and titanium alloys as a biomaterial in the field of orthopedics [1–3]. Metal-based implants tend to have a higher Young's modulus than bone, which leads to stress shielding. Calcium phosphate-based ceramics such as hydroxyapatite and calcium phosphate were obvious choices to be used in the clinics as they are components found in the native bones. Other forms of ceramics that are biocompatible such as alumina, zirconium oxide (Zirconia) and silicon oxide (silica), calcium sulphate and calcium carbonate also found their way into the clinical setting as they offer similar osteoconductive and osteoinductive properties [4–6]. In general, these bioceramics are biodegradable although at different rates depending on their composition and structure. However, a marked disadvantage of these ceramics is their brittleness [7].

* Corresponding author.
E-mail addresses: shenpa_1991@outlook.com (L. Shanmuganantha), Umar007khan@gmail.com (M.U. Aslam Khan), abubakar@ukm.edu.my (A.B. Sulong), mohdikram@ukm.edu.my (M.I. Ramli), azmibaha@ppukm.ukm.edu.my (A. Baharudin), saifulizwan@utm.my (S.I. Abd Razak), angela@ppukm.ukm.edu.my (M.H. Ng).

https://doi.org/10.1016/j.ceramint.2022.04.140
Received 2 December 2021; Received in revised form 27 March 2022; Accepted 13 April 2022
Available online 30 April 2022

Table 1
Comparison between metal and ceramic coated and composite materials.

Coated Metal Ceramic Materials		Composite Metal Ceramic Materials	
Advantages	Disadvantages	Advantages	Disadvantages
Improved wear and corrosion resistance and biocompatibility [29–31]	High temperatures prevent simultaneous incorporation of biological agents into the coating because of the decomposition and fouling of the coating caused by the residuals left after biologics decomposition [29–31]	Greatly reduces brittle fracture [32]	The final product may not be properly uniform in terms of metal and ceramic distribution [24, 33]
High interfacial adhesion strengths, and high tensile bonding strength using Ion beam-assisted deposition [29–31]	Rapid cooling produces cracks in the coating [29–31]	Mass composition of metal and ceramic can be adjusted enabling greater versatility [26, 33,34]	Some fabrications of metal and ceramics require the use of polymeric binders to mix thoroughly [26, 33,34]
Producing coating thickness ranging from 30 μm to 300 μm under Plasma spraying. Other techniques can further increase the thickness to 2 mm[29–31]	Poor control of the physicochemical parameters of the coating [29–31]	Resorption of ceramics come first from the composite material when implanted, leaving crevices on the metal portion of the composite to promote greater cell attachment afterwards [33]	Most composites can only be manufactured via powder techniques as it is the conventional method of producing the material [26, 33–36]

The bioinertness of metal-based implants also means that cells do not react to them and merely encapsulate them, and this does not promote the growth of natural tissue. Although most metals exhibit this phenomenon, ceramics such as hydroxyapatite($Ca_5(PO_4)_3(OH)$) has a similar structure to bone and helps to facilitate the growth of natural tissues. By combining metal with a ceramic, a new biomaterial can be developed to possess the ideal mechanical strength and biological properties for bone implants and osteointegration [8–14].

Titanium-hydroxyapatite has been more recently developed as a standard for most bone biomaterial implants. Conventional fabrication of this composite involves coating the ceramic to the metal base implant. It not only possesses the strength of titanium but also the bioactivity that the hydroxyapatite can exhibit which in turn provide a stable implant.

Wollastonite(CaO_3Si) is a versatile industrial mineral that is used in ceramics, cement, paints, paper and plastics [15,16]. The versatility of wollastonite has generated much interest due to its promise as a potential implantable material because it can form bonds with bone tissue through the development of a biological apatite layer on the surface [17–20]. Materials with this characteristic are known as bioactive materials and are widely used in medical and dental applications. Many studies have been performed to produce bioactive materials for various applications, such as implantable materials [21–23]. Cost-effectiveness can also be key to making materials more readily available for manufacturing and the cost of purchasing wollastonite is available in cheap commodities than other ceramic options in the market [24]. Palm stearin, which has been utilised effectively as a feedstock in earlier research, is employed as the principal binder due to its potential benefits, which include low viscosity, cheap cost, and local availability. Furthermore, palm stearin functions as a surfactant agent that can bridge between powder particles to improve feedstock homogeneity, which is critical for a successful powder injection moulding process [25, 26].

The application of wollastonite as a biomaterial is limited as not much research is done since many still prefer hydroxyapatite because of its closeness to the bone. Wollastonite is typically used in conjunction with other ceramics [7,27,28]and as for now there is very little research that shows metal and ceramic composite; be it as a coating or as a composite material. However, at this point, there are no such materials that have been fabricated that are composed of both titanium alloy and wollastonite.

Metal ceramic coating has also gained widespread attention as this is also a key point in the development of metal-ceramic biomaterials. In this case, the base component is usually made of metal and then through the use of an external coating technique; for example, plasma spraying the ceramic is then coated onto the metal and the product is ready. Table 1 shows a comparison between coated metal-ceramic materials and composite metal-ceramic materials.

In this study, two composites; one composed of both titanium alloy and hydroxyapatite and another composite composed of both titanium alloy and wollastonite were fabricated through powder compaction. This paper presents the characteristics of these composite materials through SEM, EDX, and XRD among the results to assess their physical and chemical properties as well as their mechanical strength and provides evidence of their biocompatibility with osteoprogenitor cells in vitro.

Metals and ceramics must be equally highlighted in this case as metals contain the strength to support our body and the efficiency of ceramics has their ability to generate bioactivity for the cells within their vicinity. In research conducted by Wang 2018, it is important to note that although titanium alloys and cobalt-chromium alloys have been used have been successfully used in the use of orthopaedic hip implants, there are still concerns over their clinic performance against corrosion, specially wear-assisted corrosion. Therefore, there is a growing need to involve metal implants with ceramics as standard metal-based implants seem to be less popular in promoting bone growth and regeneration [37]. Metal-based implants tend to have a higher Young's modulus than bone, which leads to stress shielding. They are also bioinert which means that cells do not react to them and merely encapsulate them, and this does not promote the growth of natural tissue [24,33].To summarize, the use of ceramics help to complement the metal's lack of bioactivity and relegate the amount of mechanical load that it presents itself to the native bone.

2. Materials & methods

2.1. Fabrication of metal-ceramic materials

Titanium alloy materials were prepared through mixing titanium allow powder TiAl6V4 where the particle size are 19.54 μm (TLS Technik GmbH & Co Spezialpulver KG) with 40% Polyethylene beads and 60% Palm Stearin which act as mixing binders at 120^{O}C using a Brabender® mixer which is then added into a metallic mould with a diameter of 15 mm and depth of 14 mm and compressed using a hot press compressor machine (Hsin Chi Machinery Co. Ltd.) at 150^{O}C and at 10 kg/m^3 which was then extruded using a hydraulic press machine (Hsin Chi Machinery Co. Ltd.) and employing a two-stage heating phase whereby the initial stage is heated up to 300^{O}C to remove the palm stearin binders and the second stage is to heat it to 500^{O}C to remove the polyethylene binders. From there it was left to cool before sintering in a vacuum sintering furnace (Korea VAC-TEC VTC 500HTSF) with a temperature of 1300^{O}C and a holding time of 2 h before cooling for 7 h. Rheological properties have already been quantified by our research counterpart and the material exhibits a pseudoplastic behaviour which is desirable for this process [26]. The resulted disc-shaped materials has

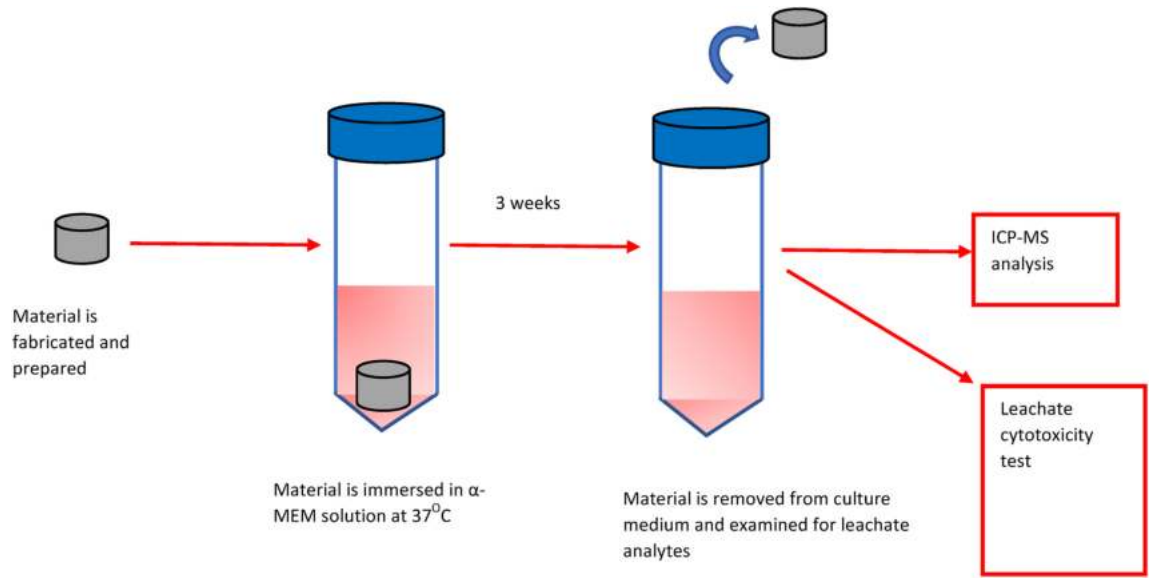

Fig. 1. Overall sequence of leachate extraction for analyte testing and cell culture testing. For this purpose, 20 ml of culture leachate was used for the materials with a surface area of 541.92 mm^2 total volume of 706.86 mm^3.

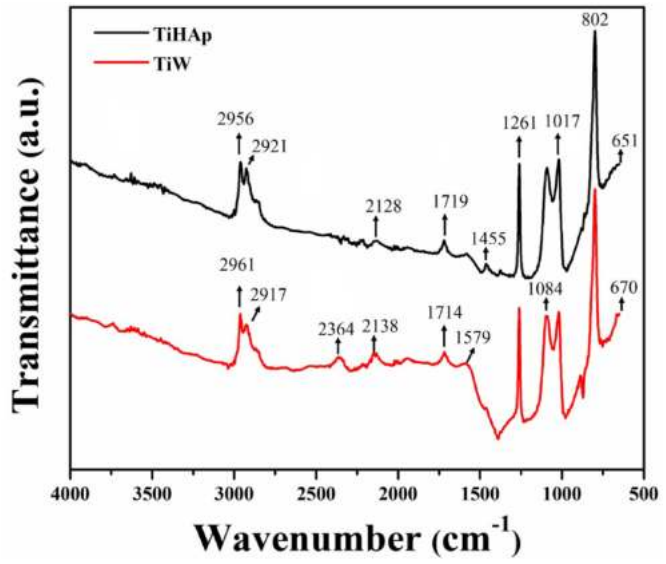

Fig. 2. Fourier Transform Imaging Spectroscopy data of Titanium Alloy-Hydroxyapatite composite, Titanium Alloy-Wollastonite composite and their control materials, Titanium Alloy, Hydroxyapatite and Wollastonite.

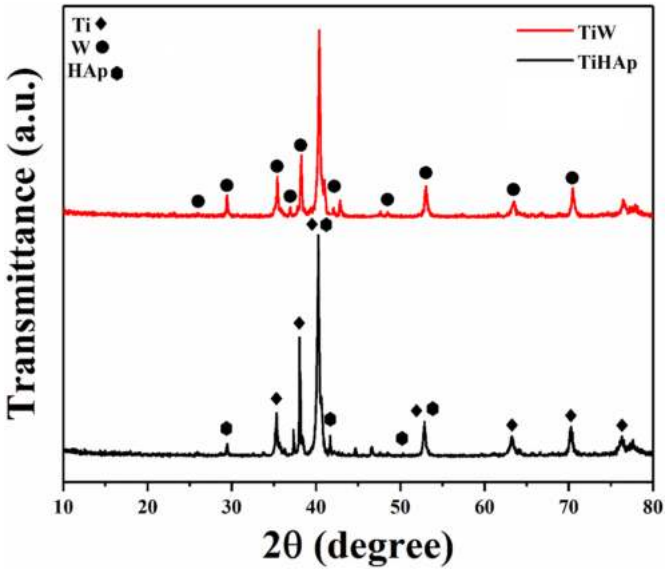

Fig. 3. XRD spectral analysis of all composite material (TiHAp and TiW).

a dimension of 15 mm in diameter and a depth of 12 mm.

The production of titanium alloy-hydroxyapatite composite materials follows the same procedure as the titanium alloy materials with a few changes. The mass composition is different as 127.44 g of titanium alloy powder is added with 14.16 g of hydroxyapatite powder(Sigma-Aldrich) with a particle size of 5 μm and it is added with 5.04 g of palm stearin and 3.36 g of polyethylene. The sintering temperature is also different with the temperature being at 1200^{O}C. All other procedures to produce the materials remains the same. The final composition by weight percentage is titanium at 90% and hydroxyapatite at 10%.

The production of titanium alloy-wollastonite materials follows the same procedure as the titanium alloy-hydroxyapatite materials with a few changes. The mass composition is different as 152.87 g of titanium alloy powder is added with 16.99 g of wollastonite powder with a particle size of 10.10 μm and it is added with 6.09 g of palm stearin and 4.06 g of polyethylene. The production of wollastonite was taken from the study by Ismail and their colleagues [19,38]. All other procedures to produce the materials remains the same. The final composition by weight percentage is titanium at 90% and wollastonite at 10%. Titanium alloy (Ti6Al4V) was used as reference material.

The materials were then cut horizontally into 3 slices; each measuring 4 mm in depth. All of the materials were cut transversely with an EXAKT 310 CP Diamond Cutter machine to reveal their surface cross-section before characterisation was carried out. Sterilization of the discs was performed via autoclaving at 121° Celsius for 20 min before biocompatibility assessments were performed.

2.2. Physicochemical characterization

2.2.1. Fourier transform infrared spectroscopy (FTIR)

The data were evaluated using a Spectrum 400 FT-IR/NIR Imaging System (PerkinElmer) from a wavelength of 600 cm^{-1} to 4000 cm^{-1} for all samples. Chemical bonds were extracted from peak references based

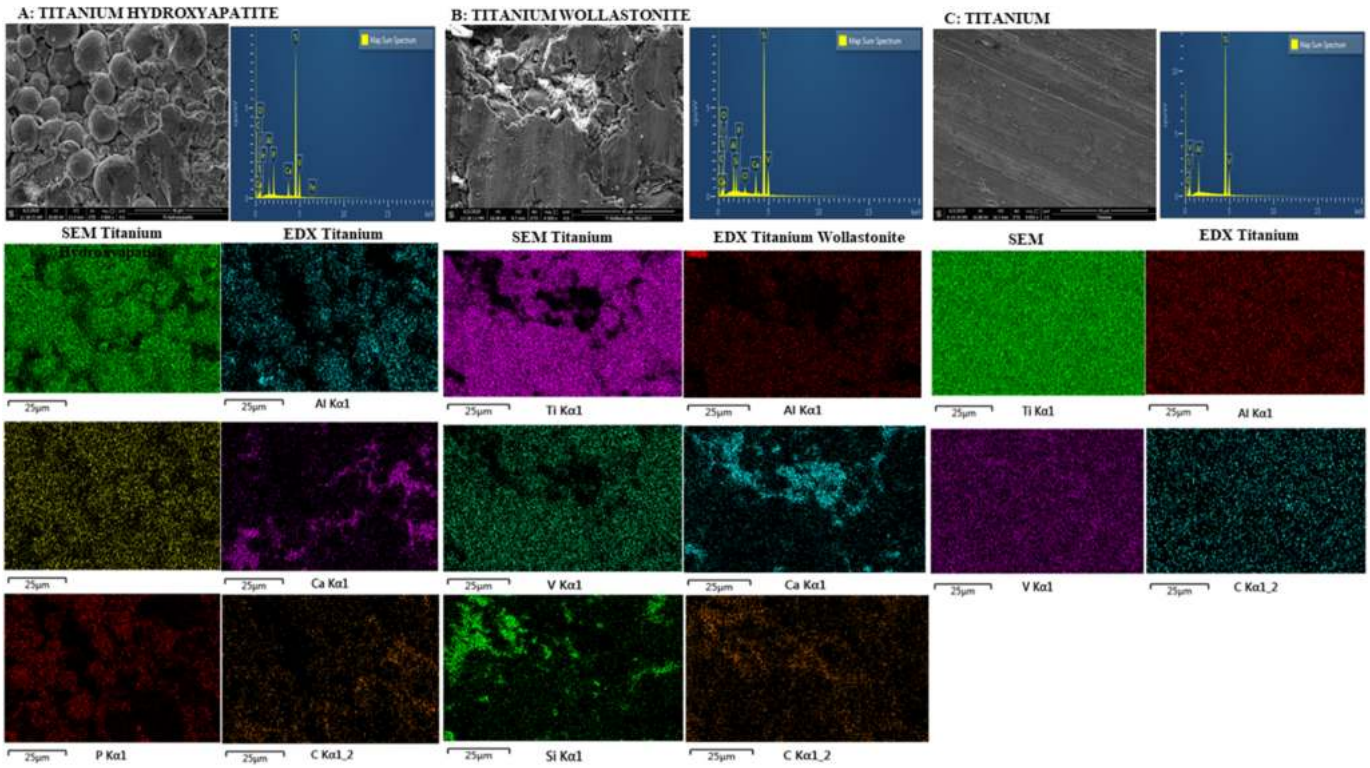

Fig. 4. SEM, EDX and EDX mapping analysis of all composite samples of TiHAp(A), TiW(B) and Titanium(C).

Table 2
Composition of key elemental components found in each titanium-ceramic material based on mass weight.

Material	Mass of element in composite(wt%)							
	Titanium	Aluminium	Vanadium	Calcium	Phosphorus	Silicon	Carbon	Oxygen
Titanium Hydroxyapatite	61.49	2.11	2.95	3.47	4.06	0	8.75	16.89
Titanium Wollastonite	53.82	3.18	2.19	3.70	0	1.94	13.09	21.01
Titanium	86.90	5.41	2.84	0	0	0	4.85	0

on the material property.

2.2.2. X-Ray diffraction spectroscopy (XRD)

XRD was carried out using the D8 Advance (Bruker) to determine the crystallinity of all materials using Cu Kα radiation, with an acceleration voltage of 40 kV and a filament current of 40 mA.

2.2.3. Scanning electron microscopy (SEM)

The images were taken using an FEI Quanta SEM and were taken in the direction of the exposed cut area of the material. The magnification of all materials was set to 1000x with a scale of 100 μm for each image.

2.2.4. 3D Laser microscopy

The surface roughness of all materials (excluding hydroxyapatite and wollastonite) was determined using the Olympus LEXT OLS5000.

2.3. Mechanical strength testing

All materials have undergone mechanical testing via Brazillian mechanical testing using Instron 8852 system. The force of compression varied among materials and was operated for approximately 5 min before the materials reached their fracture point.

2.3.1. Material leachate extraction

Material leachate was collected from all samples by immersing them in 20 ml of α-MEM solution (Gibco, USA) for three weeks in a humidified $C0_2$ incubator at 37^0C. After 3 weeks of immersion, leachate was collected and used for ICP-MS and cytotoxicity assay. Fig. 1 shows the sequence of the methodology for the extraction of the leachate.

2.3.2. ICP-MS

Two millilitres of α-MEM solution were collected and sent for Inductively coupled plasma mass spectrometry (PerkinElmer, USA) and the analyte concentrations were identified for the following elements: calcium, silicon, phosphorus, titanium, lead and mercury. A control group comprising of the α-MEM solution without any cellular intervention was also used.

2.4. Biocompatibility assessment

Primary mesenchymal stem cells derived from human bone marrow (hBMSCs) were acquired from a primary cell banking facility (CTERM, UKM, Malaysia). Cells were further expanded to passage 3 in α-MEM (Gibco, USA) supplemented with 10% fetal bovine serum (Biowest, France). Passage 3 cells were removed from the culture flasks using trypsin-EDTA (Thermo Fisher Scientific, USA) and counted using a haemocytometer for the experiments below.

2.4.1. Leachate cytotoxicity assay

Five thousand passage 3 hBMSCs were seeded onto each well of a 12-well plate. After 72 h, (approximately 70% confluency), the culture medium was replaced with 2 ml of leachate supplemented with 10%

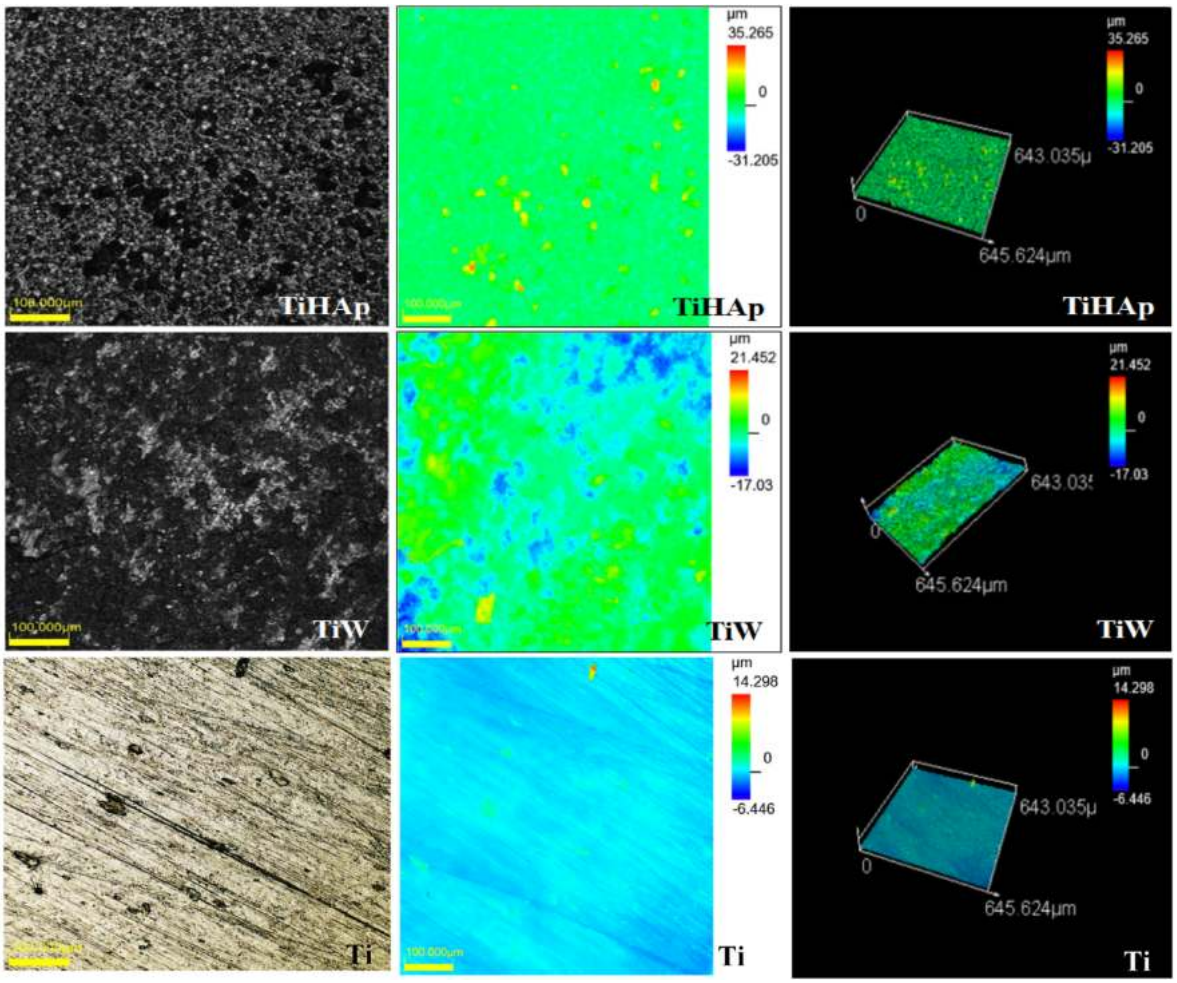

Fig. 5. 3-Dimensional Laser Microscopy of titanium hydroxyapatite (top row), titanium wollastonite (middle row) and titanium alloy (bottom row). The parameters are as follows; gross surface mapping (left column), surface mapping based on colour (centre column) and the 3D rendering of the samples (right column). (For interpretation of the references to colour in this figure legend, the reader is referred to the Web version of this article.)

fetal bovine serum. The culture medium was changed every 3 days using the leachate medium whenever necessary. PrestoBlue (Invitrogen, USA) was used to determine cell viability after 1 day, 3 days and 7 days and readings were taken by measuring the absorbance at 570 nm against 600 nm wavelengths..(PowerWave XS, BioTek, USA).

2.4.2. Assessment of the cell proliferation on the materials

hBMSCs were seeded onto the materials with a seeding density of 10000 cells/cm^2 and cultured in α-MEM + 10% FBS for another seven days. Seeded materials were then transferred to a 12-well plate and PrestoBlue (Invitrogen, USA) was used to determine cell proliferation after 1 day, 3 days and 7 days and readings were taken by measuring the absorbance at 570 nm against 600 nm wavelengths. A control group was carried out using the same primary mesenchymal stem cells cultured directly on the wall plate.

2.4.3. Assessment of the cell attachment and viability on the materials

hBMSCs were seeded onto the materials with a seeding density of 10000 cells/cm^2 for seven days After 7 days, they were stained with a Live-Dead assay kit (Invitrogen, USA) and were viewed with a fluorescence microscope (Nikon A1, Japan). A control group was carried out using the same primary mesenchymal stem cells cultured directly on the well plate using the same seeding density mentioned earlier.

3. Results and discussion

3.1. FTIR analysis

The FTIR spectrum of the bioactive composite material has shown in Fig. 2 to analyse the avail peak of the bioactive composite. As the titanium ceramic composites have similar properties to hydroxyapatite and wollastonite, they also carry similar patterns shown at the peaks stated above. The absorption bands 1084, 1017, 966, 946 and 914 cm^{-1} are due to Si–O–Si antisymmetric stretching vibration. The absorption bands at 681 and 646 cm^{-1} showed the symmetric stretching vibration of the Si–O–Si in wollastonite [39,40]. The characteristic band from 1000 to 1100 cm^{-1} confirms the calcium phosphate moiety due to wollastonite and hydroxyapatite [41]. The vibration peaks at 1084 cm^{-1} and 651 attributes to the triply degenerated P–O stretching and O–P–O bending of hydroxyapatite, respectively. Moreover, the vibration peak at 646 cm^{-1} indicates the presence of –OH that confirms the presence of hydroxyapatite. The vibration band at 646–800 cm^{-1} is a characteristic stretching vibration of TiO_2 (Ti–O) [42]. Hence, the presence of these bands confirms that our target composite material has formed.

Fig. 2 displays the FTIR spectra of the materials. The band absorption characteristics of most of the materials displayed a similar band with absorption rates at 800 cm^{-1}, 1020 cm^{-1}, 1100 cm^{-1}, 1260 cm^{-1}, and 2960 cm^{-1}. As the titanium ceramic composites have similar properties to hydroxyapatite and wollastonite, they also carry similar patterns shown at the peaks stated above. All the materials excluding titanium

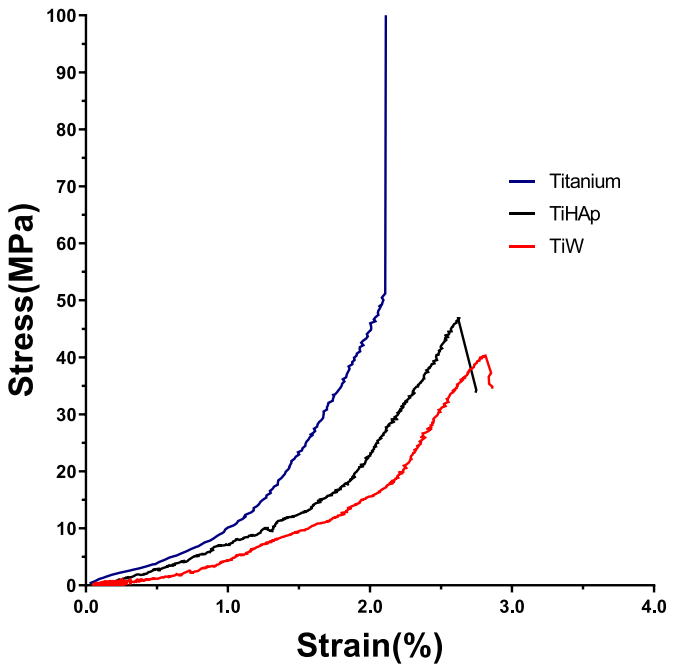

Fig. 6. Stress-strain curves of materials shown based on their recorded compressional stress until the reaching point of the material's maximum yield stress before the material is destroyed. The different colours indicate the different materials with titanium hydroxyapatite(black), titanium wollastonite (red) and titanium(blue).

Table 3
Young's Modulus of Titanium ceramic materials.

Sample	Strain (%)	Compressive Stress (MPa)	Young's modulus (GPa)
TiHAp	2.85 ± 0.75	46.86 ± 13.77	17.88 ± 4.13
TiW	2.81 ± 0.792	40.31 ± 12.10	14.34 ± 3.86
Titanium	2.71 ± 0.65	600 ± 26.53	221.40 ± 7.86

have a band peak of 1020 cm^{-1}, 1100 cm^{-1} and 1260 cm^{-1} this indicates the presence of a carbon-oxygen stretch and this is crucial to indicate the presence of non-bridging oxygen stretching modes, which are the main requirements for the initiation of the bioactive process. All materials have a significant peak at 800 cm^{-1} which indicates C–H bending formation which most likely occurred due to the sintering process at high temperatures.

3.2. Crystal structure analysis

The XRD pattern of TiHAp and TiW has been presented in Fig. 3 to determine the crystal structure. Titanium peaks dominate the composite materials followed by their respective ceramic constituents. More peaks than contained ceramic were observed within the titanium hydroxyapatite material however the silicate on the titanium wollastonite material with very low intensity. It was also diffused with other peaks that confirms the successful synthesis of composite materials. Due to the very low intensity of the peaks of the titanium hydroxyapatite, however, it is difficult to determine the phases with high confidence. As for the titanium wollastonite, apart from the major peak which is represented as titanium as that embodies 90% of the material wollastonite peaks can still be determined from the lower peak intensities with another lower intensity peak signifying the presence of quartz within the sample. The peaks of both composites are sharp due to crystalline structure and their characteristic peaks have presented in this section. The diffraction peak present at 2θ of 26.08°, 29.45°, 35.41°, 37.28°, 38.07°, 41.79°, 46.59°, 47.67°, 48.54°, 52.99° and 64.18° with their corresponding planes (002), (-2-11), (300), (022), (220), (130), (032), (222), (334), (410), and (142) [42,43]. All these peaks are attributed to the presence of hydroxyapatite and wollastonite due to the calcium phosphate structure. However, a = b = 9.4000 and c = 6.9300 are the calculated cell parameters for hydroxyapatite with a 23.29 nm average crystallite size. These parameters are perfectly matched with standard data (PDF-4-932). The corresponding diffraction peaks for the TiO_2 are 35.40°, 38.24°, 40.46°, 48.63°, 53.17°, 63.53°, 70.48° and 76.49° with (100), (002), (101), (222), (102), (110), (103), and (112) crystal planes with lattice constants a = 3.755 Å and c = 9.5114 Å [40,42]These diffraction peaks with corresponding plan confirmed the existence of the TiW composites materials. The diffused diffraction peaks were observed in composite materials at 35.50°, 38.20°, 40.37° and 53.50° composites materials. Hence, these peaks confirm the successful synthesis of our desired composite materials.

3.3. SEM/EDX analysis (Surface structure/element contribution)

The microstructures of the titanium alloy-hydroxyapatite and titanium alloy-wollastonite composites are shown in Fig. 4. Here we can see that both materials contain some form of apatite formations, which has the primary source of bone that is calcium. Unfortunately, the hydroxyapatite and wollastonite compositions within the metal-ceramic composite were not uniformly distributed within the material. This can be primarily due to the post-removal of the binders which may have left unexpected gaps within the material for the ceramic to collect during the sintering process. This was the logical inference with the assumption that the powder mixing process was homogeneous but remains an issue that needs to be addressed in the future.

Comparing them with their control material groups we can see a close similarity between titanium hydroxyapatite and the pure hydroxyapatite material. There is a presence of calcium deposit on both materials indicated by the colour mapping of calcium shown in Fig. 4 which further supports the composite benefit that the material has as if we were to compare with the standard Titanium material. The same can be said with titanium wollastonite mimicking the surface morphology of the pure wollastonite material. Table 2 provides a quantified percentage in terms of weight mass on the number of specific elements present in the titanium ceramic material as well as its control groups.

3.4. 3D Laser microscopy

Fig. 5 displays the surface characteristics of the titanium composites with the titanium alloy sample being the control element. This is primarily due to stress the importance of the significant difference in roughness as the titanium alloy gives off a roughness of 0.298 μm and titanium hydroxyapatite has a roughness of 2.550 μm which represents an 88.31% gain in roughness between the titanium sample and the metal-ceramic composite. The same can also be said for the titanium wollastonite where its surface roughness is 2.013 μm which is an 85.20% gain in roughness. This further proves the potential of metal-ceramic composites having the surface roughness needed to promote cellular adhesion and attachment.

3.5. Mechanical testing

Fig. 6 and Table 3 displays the stress-strain curves of all the materials used in this study. Titanium was recorded to have the highest compressive stress of 90.39 MPa before succumbing to fracture. The titanium hydroxyapatite and titanium wollastonite have similar stress values of 46.86 MPa and 40.31 MPa respectively. This demonstrates the composite's capability to have an improved mechanical strength This further supports the fact that the material composites can be fashioned into implants that carry a mechanical strength similar to bone.

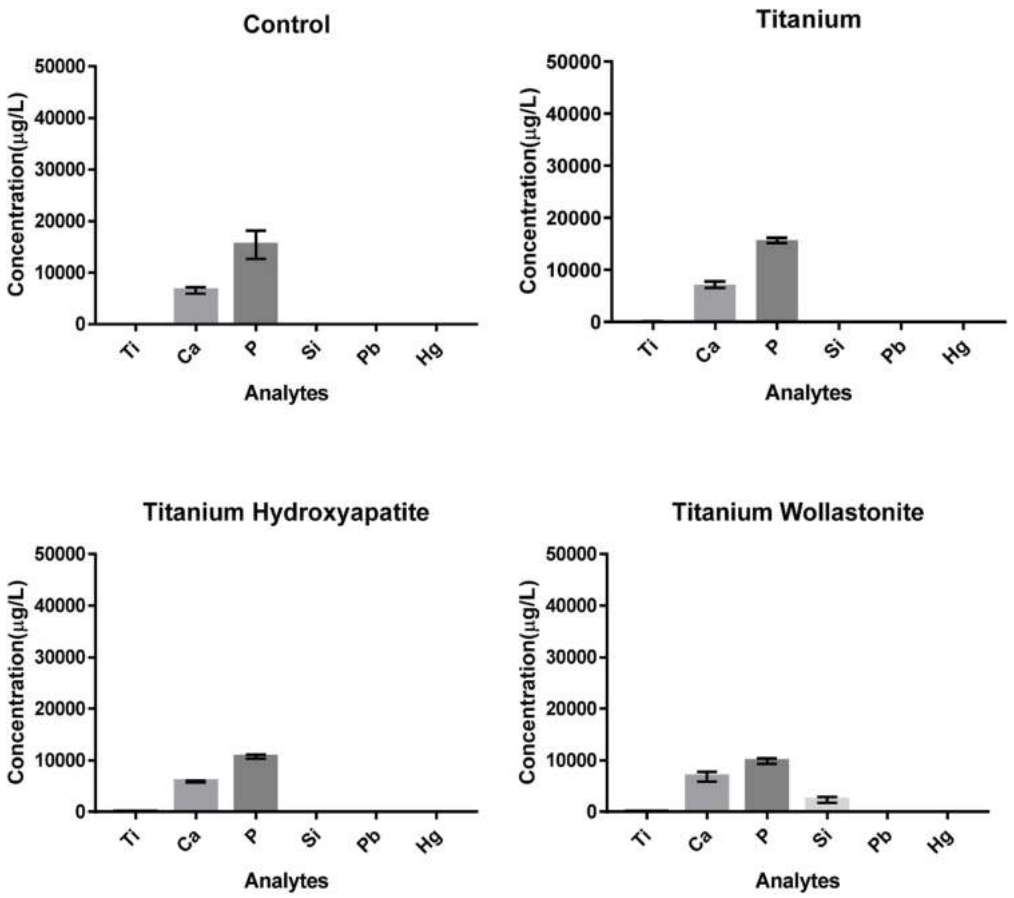

Fig. 7. Analytes present in 10 ml of material leachate carried out for 3 weeks. All analytes contained within the leachate from the materials has been normalized by the control specimen to remove the content of calcium and phosphorus that has been present within the culture medium. P-value is < 0.05.

3.6. Inductively coupled plasma mass spectroscopic analysis

Now, with regards to the cells that had been seeded onto the materials, the question arose as to whether the leachate from the material played a role in affecting the growth and proliferation of these cells. This was investigated by performing a leachate test and a mass spectroscopy analysis to identify the elements present within the materials and to determine whether these elements would harm the cells and their local environment.

3.7. Inductively coupled plasma mass spectroscopy test

Fig. 7 shows the elements present in the leachate using inductively coupled mass spectroscopy. The materials were immersed in a cell culture medium with the same contents as mentioned above, and they were stored in an incubator for 4 weeks. It is worth mentioning that all of the concentration levels of the analytes are below the upper limit of the ISO 10993-17 guidelines for allowable limits for toxic leachables which is 20 ppm or 20,000 μg/L [44].

3.7.1. Material leachate cytotoxicity assay

Fig. 8 shows the cell viability exposed to leachate extracted from materials after soaking them in a cell culture medium for 3 weeks. Our control specimen was comprised of BMSCs cultured on the well plate in standard cell culture medium. On the first day, it was observed that the control group performed significantly better than the rests, which indicate some growth inhibitory effect coming from the leachates. By day 3, the cells seemed to picked up momentum and no significant difference in cell viability was noted between all groups. On the 7th day, it could be observed that the cells exposed to leachate from titanium hydroxyapatite performed significantly poorer than the control and the titanium group. This in turn makes the titanium wollastonite an ideal candidate replacing titanium hydroxyapatite for the development of metal composite implants.

3.8. Cell proliferation or viability assay (Presto blue)

Fig. 9 shows the viability of hBMSCs that have been seeded onto the materials. It can be shown that the cells on titanium ceramic composites performed significantly better than those seeded on the base titanium material. On Day 7, the cells on titanium ceramic continued this trend and there was no statistical significance between those seeded on titanium hydroxyapatite and titanium wollastonite.

4. Live-dead assay

Fig. 10 shows the images obtained from staining the cells with the live-dead assay kit. Here, the attachment and distribution of the cells on the materials were more visible and the composite materials were shown to have good cellular attachment and viability.

5. Discussion

Concerning the importance of metals and ceramics in the composite, metals contain the mechanical strength to support our body while ceramics can generate bioactive responses from the cells within their vicinity. In today's standards, the criteria for a good biomaterial implant include both the physical properties of the bone-implant material and its ability to promote bone regeneration in the body. This is why there is a growing need to develop new implant material as a standard metal-only

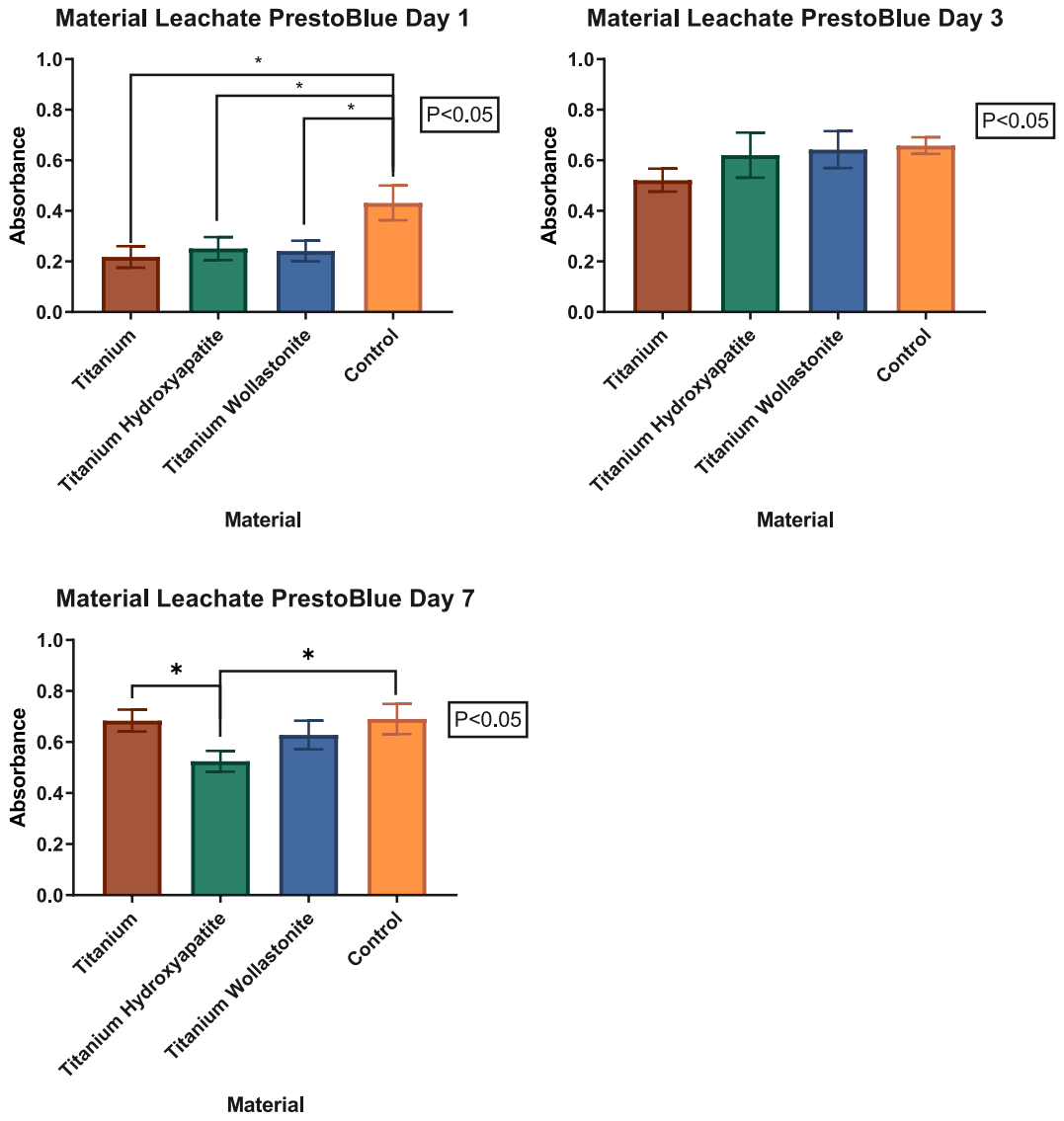

Fig. 8. Cell viability was conducted on leachate extracted from materials after soaking them in a cell culture medium for 3 weeks. All experiments were performed in biological triplicates. P-value carries a significance value of less than 0.05.

implant is ineffective in promoting bone growth and regeneration [37,45].

To balance the mechanical properties and bioactivity of materials, we would need to develop the material to be as similar as possible to the native bone. We would want to develop a composite with more titanium than ceramic as ceramics tend to increase the brittleness of the material leading to poor fabrication. Most studies have already done this with metals making up the majority component in the fabrication process [26,33,36,46]. The starting amount of ceramic that was used was 10% as our colleagues have successfully fabricated a composite material of both titanium and hydroxyapatite with hydroxyapatite at 10 wt% [26,34]. There was also an example from a previous study that by adding ceramic into the material, the material's density decreased for both titanium hydroxyapatite and titanium wollastonite [26,47]. The fabrication of titanium wollastonite was also developed to make a competitor to the aforementioned composite to gauge its effectiveness as a biomaterial. [48]As stress shielding is also a common occurrence in the usage of these metal implants which results in the loss of bone density as the mechanical load of the body has been absorbed by the implant that possesses a higher Young's modulus. Physiologically, our bones would require some form of load acting as a form of stimulus for maintaining bone tissue homeostasis and to keep its density intact. If the material's modulus is greater than that of the bone's, this would result in osteopenia [49,50] which is the very reason that the bone must be the one that maintains most of the support. From the data on the mechanical strength of the composite materials, the current composites with a 9:1 titanium to the ceramic mass ratio which has a mechanical strength of 46.86 MPa for titanium hydroxyapatite and 40.31 MPa for titanium wollastonite. Using Titanium as a comparator, however, demonstrates the wide gap between the mechanical strength of both it and the composite materials. The result of using titanium itself would have contributed to stress shielding as was described earlier. Porosity plays a critical part in this as well. As all of the materials mentioned have low porosity this means that the material has high density and our fabrication methods did not leave any room for adding any form of porosity and using MicroCT we discovered that the porosity of our materials were measured at 3%. As we are targeting the use of the implants for cortical bone, our material fits the characteristics of cortical bone which is in fact dense as well [51,52]. Temperature modification can also be key to changing the modulus of the material. This was highlighted in a study using 3 different temperatures used in the final sintering of the material which was 1100 ^{O}C, 1200 ^{O}C and 1300 ^{O}C, it was discovered that the mechanical strength of the composites decreased as the sintering temperature increased [46]. The Young's Modulus for the titanium

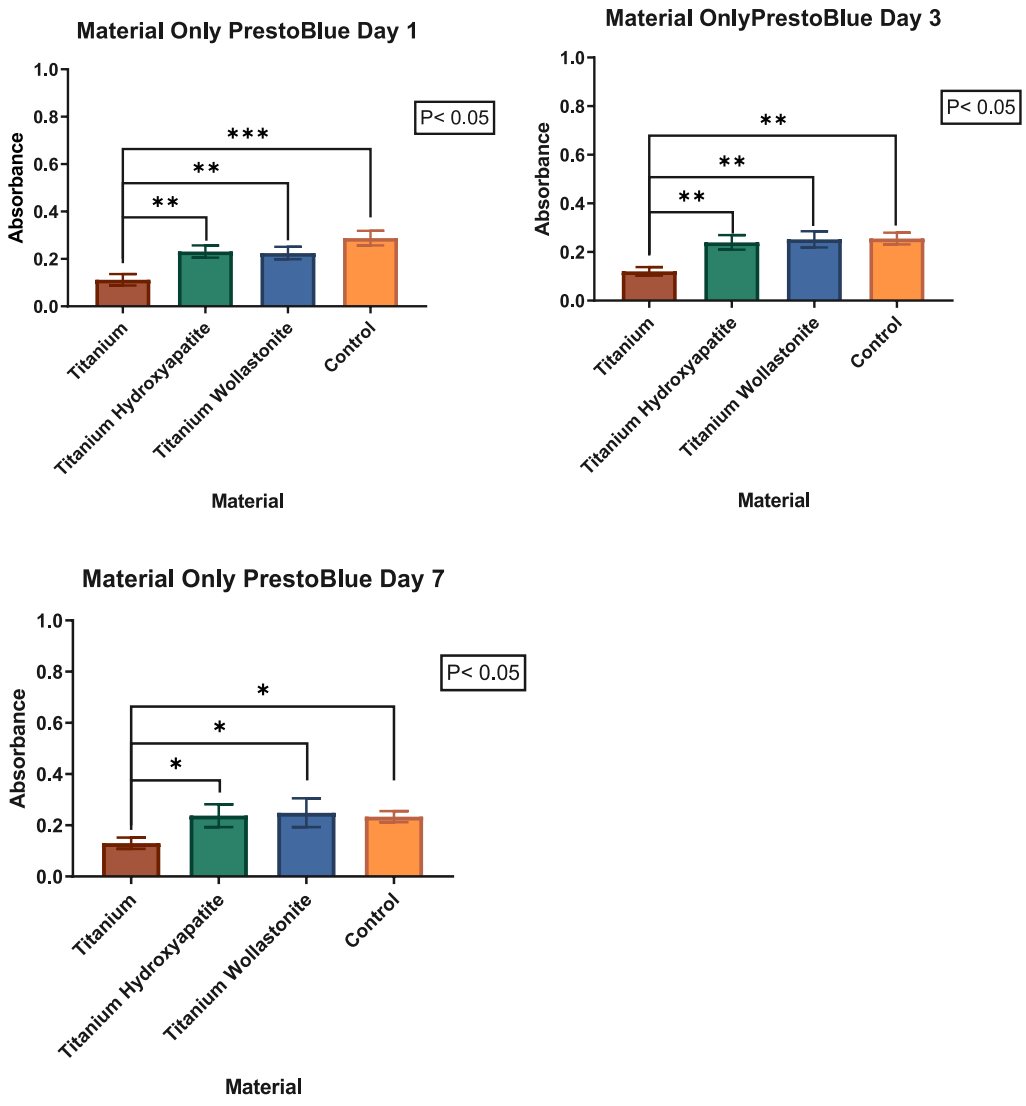

Fig. 9. Viability of stem cells seeded onto the titanium ceramic materials for 7 days. All experiments were performed in biological triplicates and carried a P-value of significantly less than 0.05.

wollastonite in the paper which was 14.57 GPa at 1300 ^{O}C is comparable to the data on the Young's Modulus of our study which was 14.34 GPa with sintering temperature at 1300 ^{O}C. From the literature, the compressive strength of human cortical bone ranges between 90 and 209 MPa [53,54] and that of the cancellous bone between 1.5 and 45 MPa [55].The compressive strength of titanium alloy is 130–170 MPa [56]. Calcium deficient HA has an average compressive strength of 174 MPa and Young's modulus of 6 GPa [55]. Based on this we can conclude that the our titanium ceramic composites are suited for cancellous bone defects but not cortical bone as the strength of cortical bone is still greater than that of the material in its current form. Comparatively, titanium wollastonite has a compressive strength and Young's modulus approximately 15% lower than titanium hydroxyapatite. Presumably, we want to strike a balance between mechanical strength and bioactivity & degradability. The composites in contrast with titanium which shows to have a significantly higher mechanical strength have a mechanical property closer to cancellous bone. This is due to the sintering temperature of the composites which were at 1300 ^{O}C. This is also further supported by other studies indicating that the higher the sintering temperature, the lower the Young's Modulus [26,34]. The concept of bone tissue engineering i.e., to develop a bone substitute that restores, maintain or improve tissue functions by incorporating (or homing in) cells, biochemical factors and a biodegradable material is deemed to be the aim of the next generation of bone implants.

For the case of the ICP Mass Spectroscopy, as shown in the results, the content of the analytes is within their recommended range as described earlier. This is important as it highlights the risks of having the implant in a setting that can contribute to blood toxicity due to the implant. Other studies have also made similar assessments using the ISO standard as well to keep the by-products of their materials which are typically leachate to an allowable limit [57–59]. Contrasting the data with the leachate viability study that was used to culture the bone marrow stem cells has further supported this statement.

In the present study, the characterisation of the titanium ceramic materials was investigated and there have been numerous similarities with other studies involving metal-ceramic materials. The FTIR, XRD, SEM and EDX data, further strengthens the importance of having rough surfaces when fabricating metal-ceramic materials. The impact of high roughness can be seen from the higher attachment of cells onto the titanium ceramic materials. From the data presented by the 3-Dimensional laser microscopy, we can see that the titanium ceramic composites have a higher roughness value than that of the titanium itself. This is mainly due to the difference in particle sizes between the metal and ceramic. Although one can argue that the titanium alloy itself is made of several metallic elements, the difference between them is not significant enough to warrant a difference as their particles are still

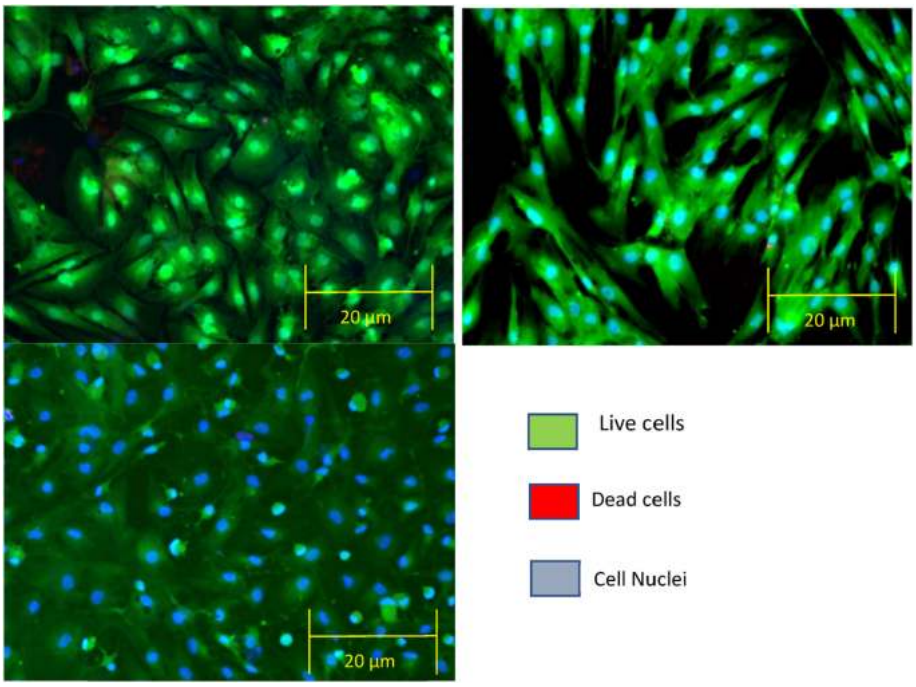

Fig. 10. Live-Dead images of cells seeded onto titanium hydroxyapatite(top), titanium wollastonite(middle) and titanium(bottom).

neatly arranged side-by-side. This is not the case for the composites however as the difference in particle sizes have created gaps thereby making its composition uneven. Other studies involving materials with high rough surfaces have also noted similar results [60]. More recently, reports on newly researched metal-ceramic composites have emerged which purport the use of a metallic matrix-like framework and then adding the ceramic component within it to fully fabricate the composite [61,62]. One study has successfully done this using Titanium Diboride powder as the filler component of the titanium matrix framework [63].

Cellular viability results show a significant increase in cellular proliferation or viability for both the titanium ceramics when compared to the titanium itself. Other studies carried out on titanium have also proved the efficiency and viability of the cells seeded onto them [64]. For the cytotoxicity tests on the material leachate, the results show that there is no significant cytotoxic effect from the leachates of the materials except for that from titanium hydroxyapatite at Day 7. Data presented in another study based on the cellular attachment on titanium wollastonite where the absorbance on Day 7 was identified as 0.32 was comparable with the data in this study which was 0.304 [25]. Bioactivity from the material also plays a role in cellular viability as the cells receive external stimulation from the material and this stimulates the mitochondria to produce more ATP creating the metabolic activity cells require to actively proliferate. Between titanium hydroxyapatite and titanium wollastonite, however, seem to have no significant difference. As our findings revealed that the distribution of the titanium and the ceramics is not evenly distributed, this would need to be improved in future for even load distribution. In addition, further tweaking of the ceramic content can be explored in future to further 'tune' the mechanical property of the composite to suit different application needs. Modification of the ceramic content within the composite can also shift the material to be more bioactive as some studies have shown that their material can be bioactive even with as little as 5% ceramic content within their composite [48].

6. Conclusion

Titanium hydroxyapatite and titanium wollastonite possess the bioactivity of ceramic while still maintaining their titanium body as a source of strength. High surface roughness and the availability of the functional groups of ceramics and the formation of apatite layer in these composites explains the satisfactory cell attachment & proliferation profile exhibited. Taken together, our data shows that the material is bioactive and predicts greater osteointegration with host bone tissue in vivo. Implantation of these composite materials in bone defects in animal models will be required next as the proof of concept. For future applications, we would propose to make this composite material into a workable scaffold as it contained promising results to be used as a bone implant.

Declaration of competing interest

The authors declare that they have no known competing financial interests or personal relationships that could have appeared to influence the work reported in this paper.

Acknowledgements

The authors would like to thank Universiti Kebangsaan Malaysia research project grants, DCP grant (DCP-2017-001/3) TRGS grant (TRGS/2/2014/UKM/02/4/2) and the university grant FF-2016-094 the PRGS grant (grant no: PRGS/1/2017/TK03/UKM/02/2) for their contribution to the creation and development of this project. Special thanks to Mr Kamalnizat Ibrahim for his assistance in procuring bone marrow samples for this study as acting medical officer of the Orthopedic and Traumatology department and the late Dr Roslinda Shamsudin from the Faculty of Science and Technology who was part of the research team of this study until she passed away some time ago whose contributions are well noted in the procurement of wollastonite for this study. Additional thanks to being given to Simon Fong Khim Mun and Kiel Tan Zi Zhang from Crest Nanosolutions Sdn Bhd. For their contributions towards the analysis of the SEM and EDX data.

References

[1] H. Lei, T. Yi, H. Fan, et al., Customized additive manufacturing of porous Ti6Al4V scaffold with micro-topological structures to regulate cell behavior in bone tissue

engineering, Mater. Sci. Eng. C (2021) 120, https://doi.org/10.1016/j.msec.2020.111789.
[2] L. Zhao, X. Pei, L. Jiang, et al., Bionic design and 3D printing of porous titanium alloy scaffolds for bone tissue repair, Compos. B Eng. 162 (2019) 154–161, https://doi.org/10.1016/j.compositesb.2018.10.094.
[3] C. Oldani, A. Dominguez, Titanium as a biomaterial for implants, in: Recent Advances in Arthroplasty, InTech, 2012, https://doi.org/10.5772/27413.
[4] S. Dorozhkin, Medical application of calcium orthophosphate bioceramics, Bio 1 (1) (2011) 1–51, https://doi.org/10.5618/bio.2011.v1.n1.1.
[5] A. Bandyopadhyay, S. Bernard, W. Xue, S. Böse, Calcium phosphate-based resorbable ceramics: influence of MgO, ZnO, and SiO 2 dopants, J. Am. Ceram. Soc. 89 (9) (2006) 2675–2688, https://doi.org/10.1111/j.1551-2916.2006.01207.x.
[6] A. Scarano, F. di Carlo, M. Quaranta, A. Piattelli, Bone response to zirconia ceramic implants: an experimental study in rabbits, J. Oral Implantol. 29 (1) (2003) 8–12, https://doi.org/10.1563/1548-1336(2003)029<0008:BRTZCI>2.3.CO;2.
[7] J.C. le Huec, T. Schaeverbeke, D. Clement+, J. Faber+, A. le Rebeller, Influence of Porosity on the Mechanical Resistance of Hydroxyapatite Ceramics under Compressive Stress, 16, 1995.
[8] K. Niespodziana, K. Jurczyk, J. Jakubowicz, M. Jurczyk, Fabrication and properties of titanium-hydroxyapatite nanocomposites, Mater. Chem. Phys. 123 (1) (2010) 160–165, https://doi.org/10.1016/j.matchemphys.2010.03.076.
[9] E.S. Thian, J. Huang, S.M. Best, Z.H. Barber, W. Bonfield, Magnetron co-sputtered silicon-containing hydroxyapatite thin films - an in vitro study, Biomaterials 26 (16) (2005) 2947–2956, https://doi.org/10.1016/j.biomaterials.2004.07.058.
[10] S. Piskounova, J. Forsgren, U. Brohede, H. Engqvist, M. Strømme, In vitro characterization of bioactive titanium dioxide/hydroxyapatite surfaces functionalized with BMP-2, J. Biomed. Mater. Res. B Appl. Biomater. 91B (2) (2009) 780–787, https://doi.org/10.1002/jbm.b.31456.
[11] E.S. Thian, N.H. Loh, K.A. Khor, S.B. Tor, Ti-6A1-4V/HA composite feedstock for injection molding, Mater. Lett. 56 (4) (2002) 522–532, https://doi.org/10.1016/S0167-577X(02)00544-X.
[12] N. Hayashi, S. Ueno, S.v. Komarov, E. Kasai, T. Oki, Fabrication of hydroxyapatite coatings by the ball impact process, Surf. Coating. Technol. 206 (19–20) (2012) 3949–3954, https://doi.org/10.1016/j.surfcoat.2012.03.066.
[13] M. Murakami, N. Nomura, H. Doi, et al., Microstructures of Zr-added Co-Cr-Mo alloy compacts fabricated with a metal injection molding process and their metal release in 1 mass% Lactic acid, Mater. Trans. 51 (7) (2010) 1281–1287, https://doi.org/10.2320/matertrans.M2010040.
[14] B. Zhang, H. Sun, L. Wu, et al., 3D printing of calcium phosphate bioceramic with tailored biodegradation rate for skull bone tissue reconstruction, Bio-Design Manufac. 2 (3) (2019) 161–171, https://doi.org/10.1007/s42242-019-00046-7.
[15] S. Vichaphund, M. Kitiwan, D. Atong, P. Thavorniti, Microwave synthesis of wollastonite powder from eggshells, J. Eur. Ceram. Soc. 31 (14) (2011) 2435–2440, https://doi.org/10.1016/j.jeurceramsoc.2011.02.026.
[16] M.M. Obeid, Crystallization of synthetic wollastonite prepared from local raw materials, Int. J. Mater. Chem. 4 (4) (2014) 79–87, https://doi.org/10.5923/j.ijmc.20140404.01.
[17] M.A. de La Casa-Lillo, P. Velásquez, P.N. de Aza, Influence of thermal treatment on the “in vitro” bioactivity of wollastonite materials, J. Mater. Sci. Mater. Med. 22 (4) (2011) 907–915, https://doi.org/10.1007/s10856-011-4254-2.
[18] X. Liu, M. Morra, A. Carpi, B. Li, Bioactive calcium silicate ceramics and coatings, Biomed. Pharmacother. 62 (8) (2008) 526–529, https://doi.org/10.1016/j.biopha.2008.07.051.
[19] H. Ismail, R. Shamsudin, M.A. Abdul Hamid, Effect of autoclaving and sintering on the formation of β-wollastonite, Mater. Sci. Eng. C 58 (2016) 1077–1081, https://doi.org/10.1016/j.msec.2015.09.030.
[20] H. Ismail, R. Shamsudin, M.A. Abdul Hamid, A. Jalar, Synthesis and characterization of nano-wollastonite from rice husk ash and limestone, in: Materials Science Forum, 756, Trans Tech Publications Ltd, 2013, pp. 43–47. 10.4028/www.scientific.net/MSF.756.43.
[21] R. Abd Rashid, R. Shamsudin, M.A. Abdul Hamid, A. Jalar, In-vitro bioactivity of wollastonite materials derived from limestone and silica sand, Ceram. Int. 40 (5) (2014) 6847–6853, https://doi.org/10.1016/j.ceramint.2013.12.004.
[22] Siriphannon P, Kameshima Y, Yasumori A, Okada K, Hayashi S. Formation of Hydroxyapatite on CaSiO 3 Powders in Simulated Body Fluid. www.elsevier.com/locate/jeurceramsoc.
[23] Lawrence Katz J, Sub Yoon H, Lipson S, et al. Calcified Tissue International the Effects of Remodeling on the Elastic Properties of Bone.
[24] L. Shanmuganantha, A. Baharudin, A.B. Sulong, R. Shamsudin, M.H. Ng, Prospect of metal ceramic (Titanium-wollastonite) composite as permanent bone implants: a narrative review, Materials 14 (2) (2021) 1–24, https://doi.org/10.3390/ma14020277.
[25] F. Fareh, V. Demers, N.R. Demarquette, S. Turenne, O. Scalzo, Influence of segregation on rheological properties of wax-based feedstocks, Powder Technol. 320 (2017) 273–284, https://doi.org/10.1016/j.powtec.2017.07.056.
[26] M.I. Ramli, A.B. Sulong, N. Muhamad, A. Muchtar, M.Y. Zakaria, Effect of sintering on the microstructure and mechanical properties of alloy titanium-wollastonite composite fabricated by powder injection moulding process, Ceram. Int. 45 (9) (2019) 11648–11653, https://doi.org/10.1016/j.ceramint.2019.03.038.
[27] C. Ohtsuki, M. Kamitakahara, T. Miyazaki, Bioactive ceramic-based materials with designed reactivity for bone tissue regeneration, J. R. Soc. Interface 6 (SUPPL. 3) (2009), https://doi.org/10.1098/rsif.2008.0419.focus.
[28] T. Kokubo, S. Yamaguchi, Novel bioactive materials developed by simulated body fluid evaluation: surface-modified Ti metal and its alloys, Acta Biomater. 44 (2016) 16–30, https://doi.org/10.1016/j.actbio.2016.08.013.
[29] R. Narayanan, S.K. Seshadri, T.Y. Kwon, K.H. Kim, Calcium phosphate-based coatings on titanium and its alloys, J. Biomed. Mater. Res. B Appl. Biomater. 85 (1) (2008) 279–299, https://doi.org/10.1002/jbm.b.30932.
[30] R.A. Surmenev, A review of plasma-assisted methods for calcium phosphate-based coatings fabrication, Surf. Coating. Technol. 206 (8–9) (2012) 2035–2056, https://doi.org/10.1016/j.surfcoat.2011.11.002.
[31] L. Sun, C.C. Berndt, K.A. Gross, A. Kucuk, Material Fundamentals and Clinical Performance of Plasma-Sprayed Hydroxyapatite Coatings: A Review, 2001, https://doi.org/10.1002/jbm.xxxx. Published online.
[32] M. Chmielewski, J. Dutkiewicz, D. Kalinski, L. Litynska-Dobrzynska, K. Pietrzak, A. Strojny-Nedza, Microstructure and properties of hot-pressed molybdenum-alumina composites, Arch. Metall. Mater. 57 (3) (2015) 687–693, https://doi.org/10.2478/v10172-012-0074-8.
[33] M.I. Ramli, A.B. Sulong, N. Muhamad, et al., Ti6Al4V/Wollastonite Composite through Powder Injection Molding Process for Bone Implant Application, 2017.
[34] A. Arifin, A.B. Sulong, N. Muhamad, J. Syarif, M.I. Ramli, HA/Ti6Al4V powder with palm stearin binder system - feedstock characterization, in: Applied Mechanics and Materials, 564, Trans Tech Publications Ltd, 2014, pp. 372–375. 10.4028/www.scientific.net/AMM.564.372.
[35] P. Divya, A. Singhal, D.K. Pattanayak, T. Rama Mohan, Injection Moulding of Titanium Metal and AW-PMMA Composite Powders, 18, 2005. http://www.sbaoi.org.
[36] A. Arifin, A.B. Sulong, N. Muhamad, J. Syarif, M.I. Ramli, Powder injection molding of HA/Ti6Al4V composite using palm stearin as based binder for implant material, Mater. Des. 65 (2015) 1028–1034, https://doi.org/10.1016/j.matdes.2014.10.039.
[37] Q. Wang, F. Eltit, R. Wang, Corrosion of orthopedic implants, in: Encyclopedia of Biomedical Engineering, 1–3, Elsevier, 2019, pp. 65–85, https://doi.org/10.1016/B978-0-12-801238-3.99863-5.
[38] M. Azmi, H. Ismail, R. Shamsudin, A. Hamid, R. Awang, Characteristics of β-Wollastonite Derived from Rice Straw Ash and Limestone, 52, 2016. https://www.researchgate.net/publication/305490553.
[39] M.U.A. Khan, H. Mehboob, S.I. Abd Razak, et al., Development of polymeric nanocomposite (xyloglucan-co-methacrylic acid/hydroxyapatite/SiO2) scaffold for bone tissue engineering applications-in-vitro antibacterial, cytotoxicity and cell culture evaluation, Polymers 12 (6) (2020), https://doi.org/10.3390/POLYM12061238.
[40] W. Chen, Y. Liang, X. Hou, et al., Mechanical grinding preparation and characterization of TiO2-coated wollastonite composite pigments, Materials 11 (4) (2018) 593, https://doi.org/10.3390/ma11040593.
[41] M. Rouahi, O. Gallet, E. Champion, J. Dentzer, P. Hardouin, K. Anselme, Influence of hydroxyapatite microstructure on human bone cell response, J. Biomed. Mater. Res. 78A (2) (2006) 222–235, https://doi.org/10.1002/jbm.a.30682.
[42] M.U.A. Khan, S. Haider, S.A. Shah, et al., Arabinoxylan-co-AA/HAp/TiO2 nanocomposite scaffold a potential material for bone tissue engineering: an in vitro study, Int. J. Biol. Macromol. 151 (2020) 584–594, https://doi.org/10.1016/j.ijbiomac.2020.02.142.
[43] M.U.A. Khan, M.A. Al-Thebaiti, M.U. Hashmi, et al., Synthesis of silver-coated bioactive nanocomposite scaffolds based on grafted beta-glucan/hydroxyapatite via freeze-drying method: anti-microbial and biocompatibility evaluation for bone tissue engineering, Materials 13 (4) (2020), https://doi.org/10.3390/ma13040971.
[44] R.P. Brown, Allowable limits for toxic leachables: practical use of ISO 10993-17 standard * *The recommendations offered in this chapter should not be construed as guidance from the US Food and Drug Administration (FDA). The mention of commercial products, their sources or their use in connection with material reported herein is not to be construed as either an actual or implied endorsement of such products by the Department of Health and Human Services, in: Biocompatibility and Performance of Medical Devices, Elsevier, 2012, pp. 95–119, https://doi.org/10.1533/9780857096456.2.95.
[45] B.E. Pjetursson, N.A. Valente, M. Strasding, M. Zwahlen, S. Liu, I. Sailer, A systematic review of the survival and complication rates of zirconia-ceramic and metal-ceramic single crowns, Clin. Oral Implants Res. 29 (2018) 199–214, https://doi.org/10.1111/clr.13306.
[46] M.Y. Zakaria, A.B. Sulong, N. Muhamad, M.R. Raza, M.I. Ramli, Incorporation of wollastonite bioactive ceramic with titanium for medical applications: an overview, Mater. Sci. Eng. C 97 (2019) 884–895, https://doi.org/10.1016/j.msec.2018.12.056.
[47] A. Arifin, A.B. Sulong, L.C. Fun, Yani I. Gunawan, Porous titanium alloy/hydroxyapatite composite using powder compaction route, J. Mech. Eng. Sci. 11 (2) (2017) 2679–2692, https://doi.org/10.15282/jmes.11.2.2017.10.0244.
[48] G.M. Peñarrieta-Juanito, M. Costa, M. Cruz, et al., Bioactivity of novel functionally structured titanium-ceramic composites in contact with human osteoblasts, J. Biomed. Mater. Res. 106 (7) (2018) 1923–1931, https://doi.org/10.1002/jbm.a.36394.
[49] M.I.Z. Ridzwan, S. Shuib, A.Y. Hassan, A.A. Shokri, Ib MN. Mohamad, Problem of stress shielding and improvement to the hip implant designs: a review, J. Med. Sci. 7 (3) (2007) 460–467, https://doi.org/10.3923/jms.2007.460.467.
[50] N. Fouda, R. Mostafa, A. Saker, Numerical study of stress shielding reduction at fractured bone using metallic and composite bone-plate models, Ain Shams Eng. J. 10 (3) (2019) 481–488, https://doi.org/10.1016/j.asej.2018.12.005.
[51] G.A.P. Renders, L. Mulder, L.J. van Ruijven, T.M.G.J. van Eijden, Porosity of human mandibular condylar bone, J. Anat. 210 (3) (2007) 239–248, https://doi.org/10.1111/j.1469-7580.2007.00693.x.
[52] D.M.L. Cooper, C.E. Kawalilak, K. Harrison, B.D. Johnston, J.D. Johnston, Cortical bone porosity: what is it, why is it important, and how can we detect it? Curr.

Osteoporos. Rep. 14 (5) (2016) 187–198, https://doi.org/10.1007/s11914-016-0319-y.
[53] J. Currey, The structure and mechanical properties of bone, in: Bioceramics and Their Clinical Applications, Elsevier, 2008, pp. 3–27, https://doi.org/10.1533/9781845694227.1.3.
[54] A.H. Burstein, D.T. Reilly, M. Martens, Aging of bone tissue: mechanical properties, J. Bone Jt. Surg. Am. Vol. 58 (1) (1976) 82–86.
[55] D.R. Carter, W.C. Hayes, The compressive behavior of bone as a two-phase porous structure, J. Bone Jt. Surg. Am. Vol. 59 (7) (1977) 954–962.
[56] R.I. Martin, P.W. Brown, Mechanical Properties of Hydroxyapatite Formed at Physiological Temperature, 6, 1995.
[57] L.C. Savery, R. Viñas, A.M. Nagy, et al., Deriving a provisional tolerable intake for intravenous exposure to silver nanoparticles released from medical devices, Regul. Toxicol. Pharmacol. 85 (2017) 108–118, https://doi.org/10.1016/j.yrtph.2017.01.007.
[58] H. Fink, N.M. de Barros Fernandes, J. Weissmann, M. Frey, Extraction with sweat-sebum emulsion as a new test method for leachables in patch-based medical devices, illustrated by assessment of isobornylacrylate (IBOA) in diabetes products, J. Diabetes Sci. Technol. 15 (4) (2020) 792–800, https://doi.org/10.1177/1932296820908656.
[59] V. Chandrasekar, D.W. Janes, C. Forrey, et al., Improving risk assessment of color additives in medical device polymers, J. Biomed. Mater. Res. B Appl. Biomater. 106 (1) (2018) 310–319, https://doi.org/10.1002/jbm.b.33845.
[60] Y. Hou, W. Xie, L. Yu, et al., Surface roughness gradients reveal topography-specific mechanosensitive responses in human mesenchymal stem cells, Small 16 (10) (2020), https://doi.org/10.1002/smll.201905422.
[61] S. Zherebtsov, M. Ozerov, M. Klimova, D. Moskovskikh, N. Stepanov, G. Salishchev, Mechanical behavior and microstructure evolution of a Ti-15Mo/TiB titanium–matrix composite during hot deformation, Metals 9 (11) (2019), https://doi.org/10.3390/met9111175.
[62] M. Motyka, Titanium alloys and titanium-based matrix composites, Metals 11 (9) (2021), https://doi.org/10.3390/met11091463.
[63] O.E. Falodun, B.A. Obadele, S.R. Oke, A.M. Okoro, P.A. Olubambi, Titanium-based matrix composites reinforced with particulate, microstructure, and mechanical properties using spark plasma sintering technique: a review, Int. J. Adv. Manuf. Technol. 102 (5–8) (2019) 1689–1701, https://doi.org/10.1007/s00170-018-03281-x.
[64] A.H. Aghajanian, A. Bigham, M. Khodaei, S. Hossein Kelishadi, Porous titanium scaffold coated using forsterite/poly-3-hydroxybutyrate composite for bone tissue engineering, Surf. Coating. Technol. 378 (2019), https://doi.org/10.1016/j.surfcoat.2019.124942.